

AD-A179 817

AN EVALUATION OF THE LOWTRAN 6 NAVY MARITIME AEROSOL  
MODEL USING 8- TO 12-MICROMETERS SKY RADIANCES(U) NAVAL  
OCEAN SYSTEMS CENTER SAN DIEGO CA H G HUGHES OCT 86

1/1

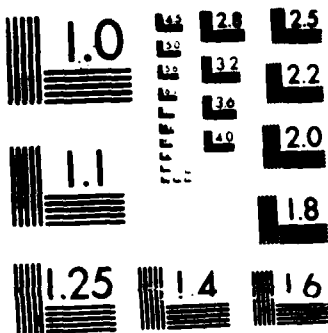
UNCLASSIFIED

NOSC/TD-1036

F/G 4/1

NL





MICROCOPY RESOLUTION TEST CHART  
NATIONAL BUREAU OF STANDARDS 1963-A

NOSC TD 1036

NOSC TD 1036

**NOSC**  
NAVAL OCEAN SYSTEMS CENTER San Diego, California 92152-5000

DTIC FILE COPY

(12)

Technical Document 1036  
October 1986

# An Evaluation of the LOWTRAN 6 Navy Maritime Aerosol Model Using 8- to 12- $\mu$ m Sky Radiances

AD-A179 817

Herbert G. Hughes

DTIC  
ELECTE  
APR 30 1987  
S D

Approved for public release; distribution is unlimited.

87 4 29 008

# **NAVAL OCEAN SYSTEMS CENTER**

**San Diego, California 92152-5000**

---

**F. M. PESTORIUS, CAPT, USN**  
Commander

**R. M. HILLYER**  
Technical Director

## **ADMINISTRATIVE INFORMATION**

This work was supported by the Office of Navy Technology Program Element 62759N, Project Number RW59-551B, over the period October 1985 to September 1986.

Released by  
H.V. Hitney, Head  
Tropospheric Branch

Under authority of  
J.H. Richter, Head  
Ocean and Atmospheric  
Sciences Division

## **ACKNOWLEDGMENTS**

Appreciation is extended to William J. Schade who made the radiance measurements available. The radiosonde measurements on board the USS *Point Loma* (AGDS-2) were provided by a Mobile Environmental Team directed by Lt. Greg A. Eisman of the Naval Oceanographic Command Facility, San Diego, CA. Programs for processing the radiosonde data were provided by Richard A. Paulus. Douglas E. Chevrier of the Pacific Missile Test Center, Pt. Mugu, CA, was responsible for the shipboard radon measurements. Appreciation is also extended to V. Ray Noonkester for many helpful discussions.

# REPORT DOCUMENTATION PAGE

1a REPORT SECURITY CLASSIFICATION <b>UNCLASSIFIED</b>			1b RESTRICTIVE MARKINGS		
2a SECURITY CLASSIFICATION AUTHORITY			3 DISTRIBUTION/AVAILABILITY OF REPORT Approved for public release; distribution is unlimited.		
2b DECLASSIFICATION/DOWNGRADING SCHEDULE					
4 PERFORMING ORGANIZATION REPORT NUMBER(S)  <b>NOSC TD 1036</b>			5 MONITORING ORGANIZATION REPORT NUMBER(S)		
6a NAME OF PERFORMING ORGANIZATION  Naval Ocean Systems Center		6b OFFICE SYMBOL (if applicable)	7a NAME OF MONITORING ORGANIZATION		
6c ADDRESS (City, State and ZIP Code)  San Diego, CA 92152-5000			7b ADDRESS (City, State and ZIP Code)		
8a NAME OF FUNDING SPONSORING ORGANIZATION  Office of Naval Technology		8b OFFICE SYMBOL (if applicable)  ONT	9 PROCUREMENT INSTRUMENT IDENTIFICATION NUMBER		
8c ADDRESS (City, State and ZIP Code)  Office of Chief of Naval Research Arlington, VA 22217-5000			10 SOURCE OF FUNDING NUMBERS		
			PROGRAM ELEMENT NO 62759N	PROJECT NO RW59-551B	TASK NO 540-SXB3
			AGENCY ACCESSION NO DN888 715		
11 TITLE (Include Security Classification)  An Evaluation of the LOWTRAN 6 Navy Maritime Aerosol Model Using 8- to 12- $\mu$ m Sky Radiances					
12 PERSONAL AUTHOR(S) H/G. Hughes					
13a TYPE OF REPORT Research		13b TIME COVERED FROM <u>Oct 1985</u> TO <u>Sep 1986</u>		14 DATE OF REPORT (Year, Month, Day) October 1986	
15 PAGE COUNT 21					
16 SUPPLEMENTARY NOTATION					
17 COSATI CODES			18 SUBJECT TERMS (Continue on reverse if necessary and identify by block number)		
FIELD	GROUP	SUB-GROUP			
			Optical scattering, Radiance algorithm		
			Atmospheric modeling, Infrared radiance		
			Aerosol size distribution Thermal imaging		
19 ABSTRACT (Continue on reverse if necessary and identify by block number)  Measurements of infrared (8-12 $\mu$ m) sky radiances over the ocean near San Diego, CA, are compared with those calculated by LOWTRAN 6 by means of the Navy Maritime Aerosol Model along with simultaneously measured (radiosonde) meteorological parameters and atmospheric radon concentrations. For a low wind-speed condition, the measured and calculated radiances agreed within 2% at the optical horizon. However, during moderate wind-speed conditions, the current wind-speed component of the aerosol model had to be lowered by factors near 20 in order to produce agreement of the calculated and measured radiances. The adjusted model is then found to agree closely with published results of large particle size distribution measurements in the North Atlantic.					
20 DISTRIBUTION AVAILABILITY OF ABSTRACT <input type="checkbox"/> UNCLASSIFIED-UNLIMITED <input checked="" type="checkbox"/> SAME AS RPT <input type="checkbox"/> DTIC USERS			21 ABSTRACT SECURITY CLASSIFICATION <b>UNCLASSIFIED</b>		
22a NAME OF RESPONSIBLE INDIVIDUAL H. G. Hughes			22b TELEPHONE (include Area Code) 225-6520		22c OFFICE SYMBOL Code 543

## CONTENTS

INTRODUCTION .....	1
MEASUREMENTS .....	2
COMPARISON OF MEASUREMENTS AND CALCULATIONS .....	3
DISCUSSION .....	11
REFERENCES .....	15

## TABLES

1 Radiosonde measurements of pressure (P, mb), temperature (T, °K), and relative humidity (REL H, %) with altitude (Z, km) taken aboard USS <i>Point Loma</i> (AGDS-2) .....	5
--	---

## ILLUSTRATIONS

1 Radiosonde measurements of temperature and relative humidity variations with altitude .....	4
2 Surface wind-speed variations with the time of day .....	6
3 Variations of atmospheric radon concentrations at sea with the time of day .....	7
4 Comparison of infrared sky radiances measured at the optical horizon with those calculated using LOWTRAN 6 .....	9
5 Sensitivity of the optical horizon sky radiances calculated with LOWTRAN 6 using the Navy Maritime Aerosol Model with differing surface wind-speed parameters .....	10
6 Examples of aerosol size distributions calculated with different values of the multiplying factor k .....	12
7 Comparisons of measured particle size distributions with those calculated with the original and adjusted Navy Maritime Aerosol Model .....	13
8 Values of the current wind-speed multiplying factor k required to obtain agreement between measured and calculated radiances and particle size distributions .....	14



Accession For	
NTIS CRA&I	<input checked="" type="checkbox"/>
DTIC TAB	<input type="checkbox"/>
Unannounced	<input type="checkbox"/>
Justification	
By	
Distribution /	
Availability Codes	
Dist	Avail and/or Special
A-1	

## INTRODUCTION

The primary factors affecting infrared electro-optical surveillance, guidance and weapon systems in the marine environment are atmospheric water vapor and aerosols which absorb and scatter the radiation. In the absence of real-time measurements, we must presently rely on the LOWTRAN 6 atmospheric propagation code<sup>1</sup> to predict infrared transmission losses and sky backgrounds, using as inputs measured meteorological parameters. The effects of water vapor absorptions are adequately handled by LOWTRAN 6, and selectable size distribution models are available for calculating the aerosols' absorption and scattering properties. One of these aerosol models (Navy Maritime Model), which is applicable to ocean atmospheres, was developed by Gathman<sup>2</sup> at the Naval Research Laboratory, utilizing a large data set of size distributions and meteorological parameters measured near the surface in a variety of marine environments. The particle size distribution model (at radius  $r$ ) is the sum of three log-normal distributions given by

$$n(r) = \sum_{i=1}^3 A_i \exp \left[ -\left( \frac{\ln r}{f r_i} \right)^2 \right], \text{ cm}^{-3} \mu\text{m}^{-1}, \quad (1)$$

where

$$A_1 = 2000 (\text{AM})^2 \quad (2a)$$

$$A_2 = 5.866 (\bar{v} - 2.2) \quad (2b)$$

$$A_3 = 0.01527 (v_c - 2.2) \quad (2c)$$

Component one represents the contribution by continental aerosols. (AM) is an air mass parameter which varies between integer values of 1.0 for open ocean to 10 for coastal areas given by

$$(\text{AM}) = Rn/4 + 1, \quad (3)$$

where  $Rn$  is the measurement of atmospheric radon content expressed in picocuries per cubic meter ( $\text{pCi}/\text{m}^3$ ). Components two and three represent equilibrium sea spray particles generated by the 24-hour averaged ( $\bar{v}$ ) and current ( $v_c$ ) surface wind speeds in meters per second. In Eq. (2b), if  $5.866(\bar{v} - 2.2) < 0.5$ , then  $A_2 = 0.5$ ; and in Eq. (2c), if  $0.01527(v_c - 2.2) < 1.5 \times 10^{-5}$ , then  $A_3 = 1.5 \times 10^{-5}$ .

In Eq. (1),  $r_i$ , the modal radius for each component, is allowed to grow with relative humidity (RH) according to

$$f = \left[ \frac{2 - \text{RH}/100}{6(1 - \text{RH}/100)} \right]^{1/3} \quad (4)$$

The contribution to the total extinction or absorption by each aerosol component can be written as

$$\beta_{e,a}(\lambda)_i = C_i \int_r Q_{e,a}(\lambda, r, m) \exp \left[ -\left( \frac{\ell n r}{f r_i} \right)^2 \right] r^2 dr, \quad (5)$$

where  $C_i = \frac{0.001\pi}{f} (A_i)$ . The factor  $f^{-1}$  in the expression for  $C_i$  insures a constant total number of particles as the relative humidity increases.  $Q_{e,a}(\lambda, r, m)$  is the cross section for either extinction or absorption normalized to the spherical-particle geometrical cross section, and  $m$  is the complex refractive index, which is allowed to change from that of dry sea salt as the particle deliquesces with increasing humidity. LOWTRAN 6 provides precalculated values in tabular form of the parameter  $\beta_{e,a}(\lambda)_i/C_i$  at discrete wavelengths and four relative humidities (50, 85, 90 and 99%), from which the average extinction or absorption coefficient for a specific wavelength band and relative humidity can be readily determined by interpolation between the stored values. When an observed surface visual range (visibility) is available as an input to the model, the amplitudes of the three components will be adjusted so that the calculated visual range at a wavelength of  $0.55 \mu\text{m}$  is the same as the observed value.

The accuracy to which this model can predict infrared extinction coefficients has been tested only against a limited set of surface transmissometer and meteorological measurements at San Nicolas Island<sup>3</sup>. Good correlations between calculated and measured extinctions for wavelengths of  $1.06 \mu\text{m}$  and  $3.6 \mu\text{m}$  were obtained. At  $10.5 \mu\text{m}$  the agreement was less, with the calculated extinctions being 20 to 40% greater than those measured by the transmissometer. These correlations, however, were sensitive to the selection of the air mass factor and whether or not the visibility was used as an input. An alternative approach is to test the model's utility to predict the infrared radiance of the sky. It is well known<sup>4</sup> that the absorption (and emissivity) of the atmosphere for the 8- to  $12\text{-}\mu\text{m}$  wavelength band depends on the optical path length such that the effective blackbody temperature of the sky will increase with the zenith angle. Near the horizon, the sky temperature will equal the ambient air temperature unless aerosols, which scatter the radiation, are present. The effects of aerosols for this wavelength band, however, are noticeable only at zenith angles greater than about  $85^\circ$  (in cloud-free skies). In this paper, we examine the utility of the aerosol model (with the LOWTRAN 6 radiance algorithm) to predict infrared (8 -  $12 \mu\text{m}$ ) sky radiances which were measured close to the horizon simultaneously with radiosonde measurements of meteorological parameters. For this to be a valid approach, we must rely upon the accuracies of the measurements and the LOWTRAN 6 radiance algorithm.

## MEASUREMENTS

The infrared (8 -  $12 \mu\text{m}$ ) sky radiances for these investigations were obtained on 16 April 1986. The measurements were made with a calibrated thermal imaging system (AGA THERMOVISION, Model 780) using a  $2.95^\circ$  field-of-view (FOV) lens with an instantaneous field-of-view (IFOV) of  $0.9 \text{ mrad}$ . The response of each wavelength band is determined by placing a blackbody of known temperature ( $\pm 0.1^\circ \text{C}$  for temperatures  $< 50^\circ \text{C}$ ) close to the aperture of the lens. The digitized video signal transfer function of the system then allows the blackbody temperature to be reproduced to within  $0.2^\circ \text{C}$ . The video output of the scanner is digitized and processed on a microcomputer to allow the temperature of selected pixels of the scene



to be displayed. For these measurements the scanner was directed due west over the ocean from an altitude of 33 m such that approximately 2° of the FOV was above the horizon. During the recording period, radiosondes were launched from a ship (USS *Point Loma* (AGDS-2)) 5 km off the coast of Pt. Loma, San Diego, CA. The radiosonde system employed was the VAISALA model RS80. The measured temperature and relative humidity variations with altitude for three periods 0845, 1245 and 1645 PST 16 April) are graphically shown in Fig. 1 and tabulated with the pressure variations in Table 1. During the first launch, broken stratus clouds were present near an elevation of 900 m. During the subsequent launches, the clouds persisted, but the coverage was scattered. Surface wind speeds and directions were recorded continuously on shore at the sensor site and periodically aboard the ship. Northwesterly winds ( $310^\circ \pm 10^\circ$ ) had persisted for 24 hours prior to and during the measurements with varying speeds as shown in Fig. 2. At 0800 PST on 16 April the wind speed had increased from approximately 3 m/s to values between 9 m/s and 12 m/s. The 24-hour average and current wind speeds coinciding with the times of the radiosonde launches are tabulated in the figure. Measurements of atmospheric radon were also made aboard the USS *Point Loma* to aid in determining the air mass characteristics. The radon counts measured as a function of time are shown in Fig. 3 and indicate the air mass was primarily of maritime origin ( $<4$  pCi/m<sup>3</sup>) throughout the measurement period. The increased radon counts near 0400 PST on 15 April coincide with the in-port time of the ship.

## COMPARISON OF MEASUREMENTS AND CALCULATIONS

The LOWTRAN 6 radiance algorithm assumes the atmosphere to be composed of a number ( $n_{\max} = 33$ ) of isothermal layers characterized by a temperature  $T_i$  and spectral transmittance  $\tau(\lambda, i, \theta)$  along the optical path traversing the  $i^{\text{th}}$  layer at angle  $\theta$ . From Kirchoff's law, the spectral radiance of the  $i^{\text{th}}$  layer is

$$N(\lambda, i, \theta) = \left[ 1 - \tau_a(\lambda, i, \theta) \right] \frac{B(\lambda, T_i)}{\pi}, \quad (6)$$

where  $\tau_a(\lambda, i, \theta)$  is the absorption transmittance and  $B(\lambda, T_i)$  is Planck's blackbody radiation formula. Then the spectral radiance reaching the ground through the intervening atmosphere

$$N(\lambda, i, \theta) \prod_{j=1}^{i-1} \tau(\lambda, j, \theta) = \left[ 1 - \tau_a(\lambda, i, \theta) \right] \left[ \prod_{j=1}^{i-1} \tau(\lambda, j, \theta) \right] \frac{B(\lambda, T_i)}{\pi}. \quad (7)$$

Summing up the contribution from all layers, the spectral radiance reaching the ground is

$$N(\lambda, \theta) = \sum_{i=1}^n \left[ 1 - \tau_a(\lambda, i, \theta) \right] \left[ \prod_{j=1}^{i-1} \tau(\lambda, j, \theta) \right] \frac{B(\lambda, T_i)}{\pi}, \quad (8)$$

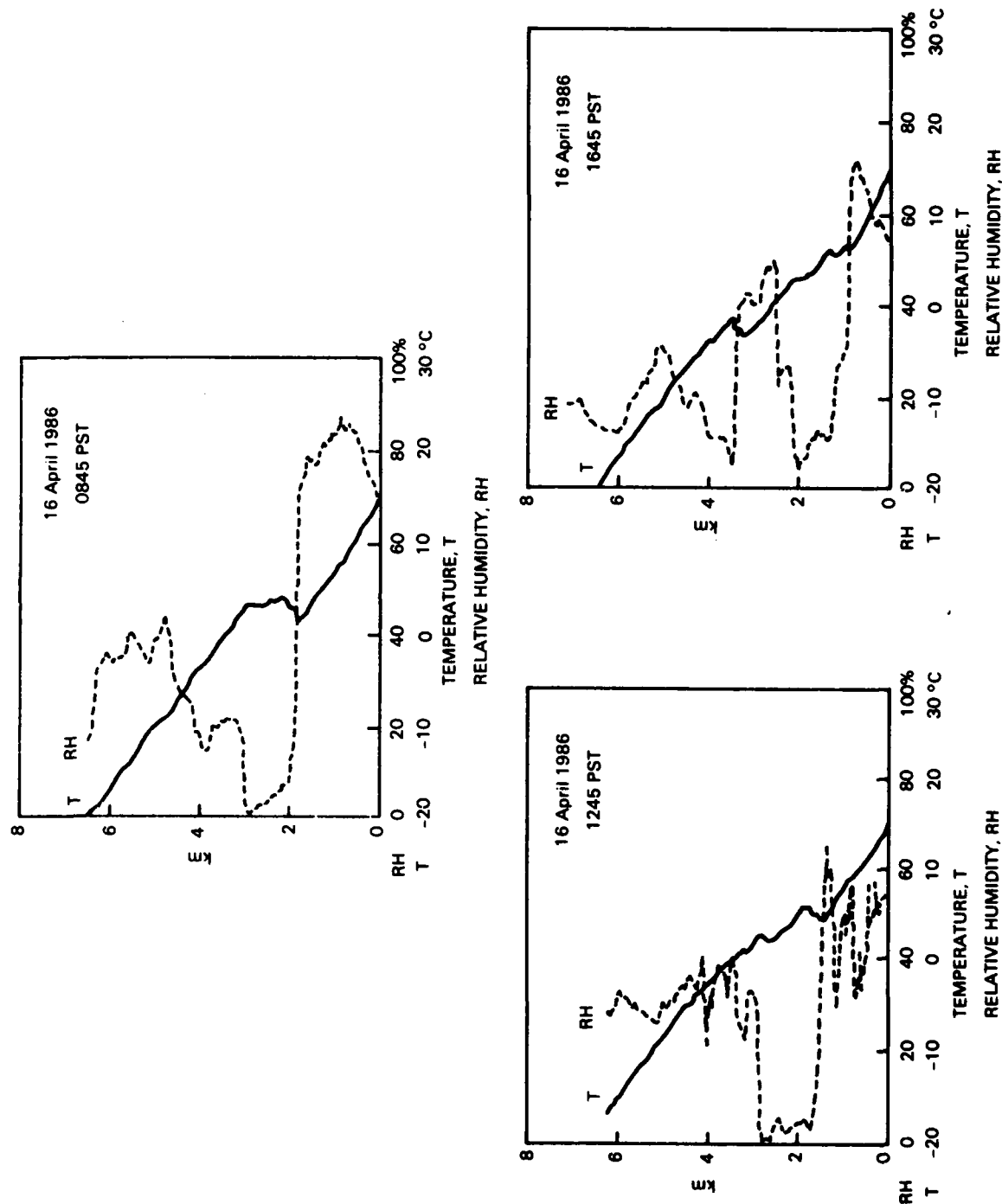


Figure 1. Radiosonde measurements of temperature and relative humidity variations with altitude.

Table 1. Radiosonde measurements of pressure (P, mb), temperature (T, °K), and relative humidity (REL H, %) with altitude (Z, km) taken aboard USS Point Loma (AGDS-2)

16 April 1986 0845 PST				16 April 1986 1245 PST				16 April 1986 1645 PST			
Z (KM)	P (MB)	T (K)	REL H (%)	Z (KM)	P (MB)	T (K)	REL H (%)	Z (KM)	P (MB)	T (K)	REL H (%)
.008	1014.800	288.55	65.00	.008	1017.700	288.65	50.00	.008	1016.100	288.85	50.00
.068	1007.600	287.55	70.00	.083	1008.700	287.55	54.00	.083	1007.100	287.25	54.00
.143	998.700	286.85	73.00	.158	999.700	286.75	54.00	.143	999.900	286.55	56.00
.219	989.800	286.25	75.00	.233	990.900	286.25	52.00	.233	989.300	285.75	58.00
.308	979.300	285.45	78.00	.264	987.400	286.05	54.00	.308	980.600	285.25	58.00
.428	965.400	284.45	81.00	.338	978.600	285.25	50.00	.413	968.400	284.25	60.00
.532	953.500	283.45	84.00	.457	964.800	284.35	49.00	.427	966.700	284.05	58.00
.650	940.000	282.45	86.00	.590	949.400	283.35	35.00	.575	949.600	282.55	66.00
.783	925.100	281.45	86.00	.650	942.700	283.25	31.00	.722	932.900	281.25	71.00
.843	918.500	280.95	86.00	.724	934.300	282.75	36.00	.738	931.200	281.05	71.00
.901	912.000	280.75	86.00	.798	926.100	282.45	57.00	.869	916.400	279.95	71.00
1.018	899.100	280.15	84.00	.856	911.500	282.05	49.00	.885	914.800	279.75	71.00
1.123	889.500	279.45	83.00	.931	911.300	281.75	48.00	.957	906.700	279.45	54.00
1.225	878.500	278.75	81.00	.960	908.100	281.55	49.00	.987	903.400	279.75	31.00
1.356	864.500	277.95	80.00	1.034	900.000	280.75	48.00	1.015	900.200	279.75	30.00
1.458	853.800	277.15	78.00	1.122	890.500	280.25	32.00	1.177	882.800	278.95	28.00
1.544	844.800	276.45	78.00	1.384	862.400	278.15	63.00	1.323	867.200	279.25	13.00
1.629	834.300	275.85	78.00	1.515	848.700	277.75	23.00	1.483	850.400	279.15	11.00
1.773	819.600	274.95	72.00	1.689	830.700	278.45	4.00	1.860	811.900	276.75	9.00
1.903	806.500	276.15	15.00	2.412	760.000	275.95	5.00	2.062	791.900	276.25	6.00
2.047	792.300	277.35	8.00	2.700	733.400	275.15	1.00	2.292	769.700	275.65	26.00
2.957	708.200	276.65	2.00	2.843	720.400	275.65	4.00	2.422	757.400	274.85	26.00
3.087	697.000	275.45	20.00	2.930	712.800	274.95	32.00	2.522	748.000	274.15	23.00
3.658	649.100	271.85	21.00	3.102	697.700	273.85	32.00	2.622	738.800	273.45	50.00
3.899	629.700	270.25	16.00	3.159	692.800	273.95	24.00	2.964	707.900	271.65	41.00
4.292	599.100	268.05	25.00	3.330	678.100	273.35	26.00	3.261	681.900	270.15	42.00
4.612	575.000	265.05	33.00	3.459	667.300	272.85	39.00	3.444	666.300	270.65	40.00
4.778	562.900	264.25	43.00	3.729	645.100	271.45	37.00	3.558	656.900	271.85	7.00
5.149	536.500	262.75	35.00	4.040	620.400	270.05	26.00	4.094	613.900	269.55	11.00
5.531	510.400	259.45	40.00	4.152	611.600	269.35	36.00	4.569	577.800	266.75	19.00
				5.085	542.800	264.05	27.00	5.149	536.200	262.45	32.00
				5.687	501.900	260.25	28.00	5.286	526.700	262.05	26.00
								5.653	502.000	259.75	21.00

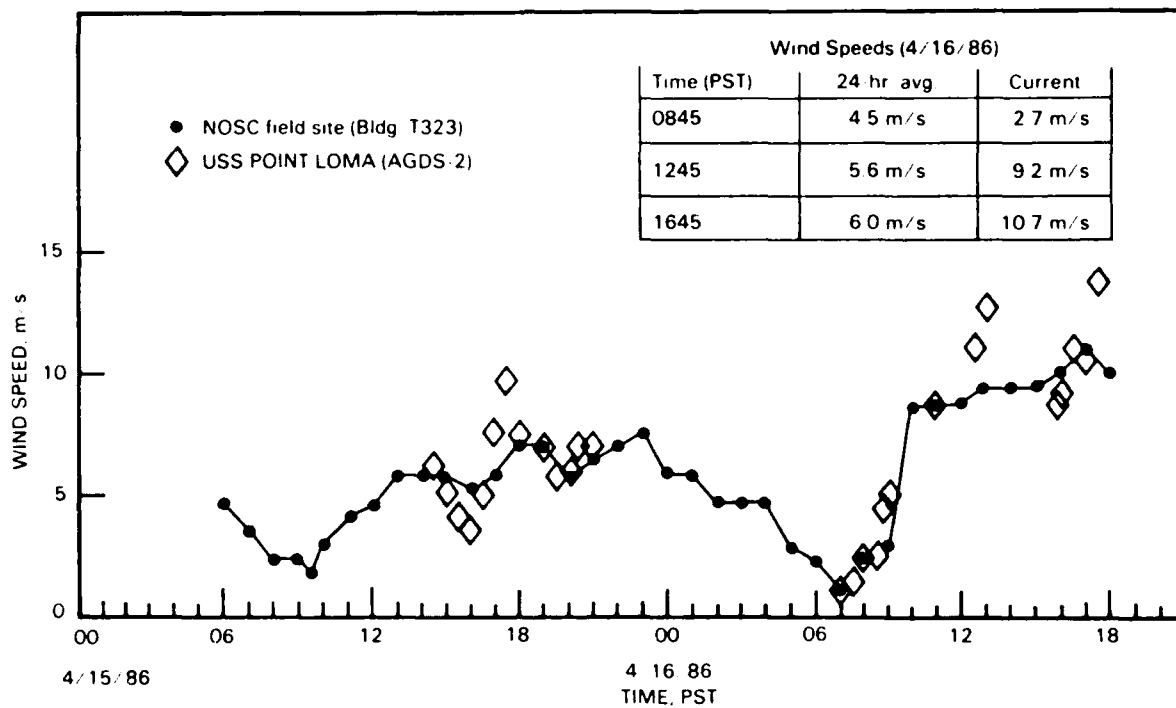


Figure 2. Surface wind-speed variations with the time of day.

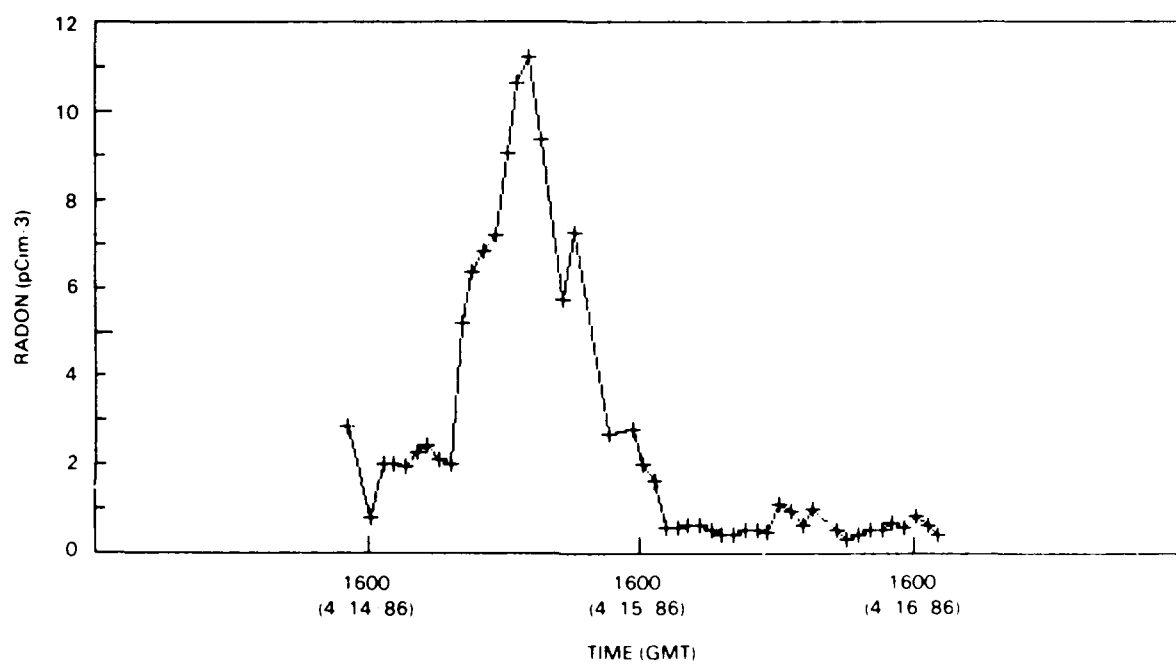


Figure 3. Variations of atmospheric radon concentrations at sea with the time of day.

In this equation, scattering is considered only as a loss mechanism through the extinction transmittance term  $\exp(-\tau(\lambda, \theta))$  and is not included as a source of radiation. It has been proposed by Ben Shalom et al.<sup>7</sup> that the LOWTRAN algorithm was deficient, i.e., multiple scattering effects over the long propagation paths affecting the sky radiance were not properly addressed. They proposed a modification to LOWTRAN to include scattering as a source of radiation by replacing the absorption transmittance in Eq. (8) by the extinction transmittance. However, utilizing data similar to that herein, Hughes et al.<sup>8</sup> have shown that the proposed conservative scattering modifications to LOWTRAN grossly overestimate the horizon sky radiances when aerosols are present and that multiple scattering effects are negligible, at least for the wavelength band and atmospheric conditions considered.

In Fig. 4, the sky radiances measured at the optical horizon (zenith angle,  $\theta = 90.17^\circ$ ) are compared to those calculated using the unmodified LOWTRAN 6 code with the measured meteorological data. We have chosen to address only the sky radiance at the optical horizon because of the possible contamination of the measurements by the scattered stratus clouds. (It can be shown<sup>7</sup> that  $8 - 12 \mu\text{m}$  radiances at the optical horizon are insensitive to cloud emissions because of the low atmospheric transmittances over the contributing optical path lengths.) The clear-air radiance calculations were made using plus and minus uncertainties ( $0.5^\circ\text{C}$  in temperature and 5% in relative humidity) as shown. In each case, the clear-air calculations are greater than the measurements, indicating a small presence of aerosols. (These radiance differences correspond to equivalent blackbody temperature differences of 2 to  $3^\circ\text{C}$ .) The calculations made with the Navy Maritime Aerosol Model were for an air mass factor of unity for maritime air (as indicated by the radon measurements) and the 24-hour average and current surface wind speeds as listed in Fig. 2. In the first case there is good agreement between the measured and calculated radiances. By adjusting the surface visibility input to 130 km (as compared to the default value of 96.8 km) the calculated radiance can be made to coincide with the measured value. For the second and third time periods, the calculations differ greatly from the measurements by equivalent blackbody temperatures of approximately  $15^\circ\text{C}$  and  $20^\circ\text{C}$ , respectively. The calculations can be made to agree with the measurements by adjusting the default visibilities of 31 km and 35 km to values of 180 km and 210 km, respectively. These visibilities are excessive, based on visual observations of coastal islands at the time of the measurements. Los Coronados Islands ( $\sim 30$  km distant) were clearly seen. However, San Clemente Island with a peak elevation of  $\sim 600$  m was not visible from the upper decks of the USS *Point Loma* at a distance of 75 km. In the  $8 - 12 \mu\text{m}$  band, the horizon radiance is affected mainly by the aerosols with radii greater than  $1 \mu\text{m}$ , which scatter the radiation. The comparison discrepancies in Fig. 4 most likely stem from the current wind speed component, which determines the number of particles greater than  $1 \mu\text{m}$ . This wavelength band is less likely to be influenced by the 24-hour average wind-speed component, which mainly generates particles in the  $0.1$ - to  $1\text{-}\mu\text{m}$  radius interval. In Fig. 5, the relative sensitivity of the radiance calculations to the wind-speed factors is demonstrated by means of the 1645 PST data set. The radiance calculations are insensitive to 24-hour wind speeds varying between 2.2 m/s and 10 m/s, but are extremely sensitive to the current wind speed. If the multiplying constant in Eq. (2c), ( $k = 0.01527 \text{ s/m}$ ), and a 24-hour average wind speed of 6.0 m/s are maintained, the current wind speed must be reduced to 2.6 m/s to obtain agreement between calculated and measured radiances. If the measured value of current wind speed is to

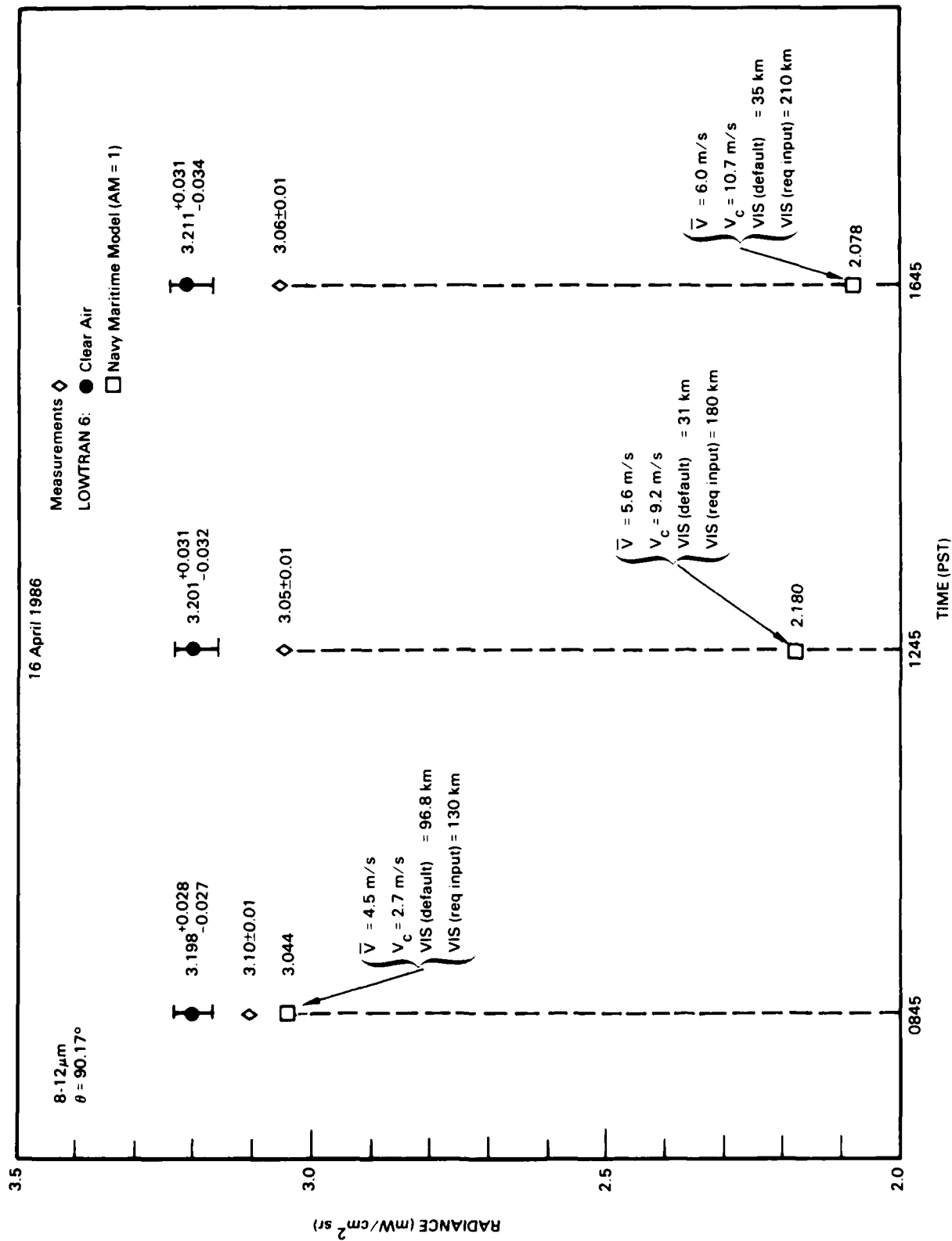


Figure 4. Comparison of infrared sky radiances measured at the optical horizon with those calculated using LOWTRAN 6.

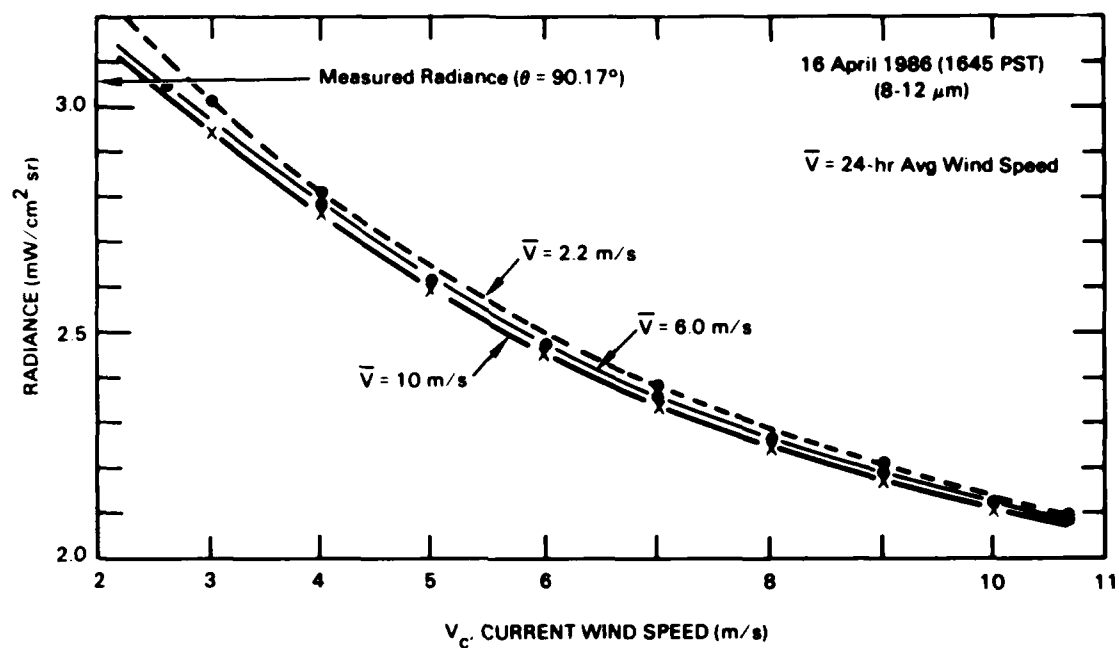


Figure 5. Sensitivity of the optical horizon sky radiances calculated with LOWTRAN 6 using the Navy Maritime Aerosol Model with differing surface wind-speed parameters.



be maintained in the LOWTRAN calculations, the multiplying constant,  $k$ , must be reduced by a factor near 20 to 0.0007 s/m. The size distributions associated with the different values of  $k$  are shown in Fig. 6. For particle radii less than 1  $\mu\text{m}$ , the size distributions are unaffected by changes in  $k$ . At larger radii, the size distribution for  $k = 0.0007$  s/m are smaller by an order of magnitude. This reduction in the number of larger particles accounts for the increase in the calculated radiance, i.e., the scattering losses are reduced.

Recently, published results by Dee Leeuw<sup>8</sup> of large particle size distributions ( $r > 5 \mu\text{m}$ ) in the North Atlantic provide another method of evaluating the current wind-speed component in the present model. In that work, size distributions were measured with an impactor at different heights (0.2 to 11 m) above the sea surface. Measured size distributions (normalized to a relative humidity of 80% according to the formulas of Fitzgerald<sup>9</sup>) were graphically presented for an altitude of 11 m as a function of surface wind speed. Here, size distributions were calculated with the model, using the measured surface meteorological parameters and the  $k$ -factor in the original model was adjusted to obtain agreement with those presented by Dee Leeuw (after adjustment to the average measured relative humidity in the first two radiosonde levels). An example of the comparisons is shown in Fig. 7 for the 1645 PST set of data. Excellent agreement between the adjusted and measured size distribution is obtained for a  $k$ -factor of 0.00109 s/m. This value is approximately 36% higher than that determined from the radiance measurements. The difference may reflect the assumption in the present model that the number of surface-generated particles remains constant up to an altitude of 2 km, where the LOWTRAN 6 calculations default to the Tropospheric Aerosol Model. However, it can be shown that the radiance calculations at the optical horizon are affected less than 2% by including only the lowest two levels of the radiosonde profile. The  $k$ -factors determined by both techniques are shown in Fig. 8 at the measured wind speeds. Within the measurement accuracies of both techniques and those to which the size distributions could be scaled from the graph in Dee Leeuw's paper, the  $k$ -factors can be considered to be in reasonable agreement.

## DISCUSSION

It is interesting to notice in Fig. 6 the suggestion of a linear dependency of the factor  $k$  on the current wind speed. However, because of the small data sample, no quantitative conclusions can be made in this regard.

A joint effort by the Naval Research Laboratory, the Naval Postgraduate School, and the Naval Ocean Systems Center is presently underway to develop a Navy Ocean Vertical Aerosol Model (NOVAM) for inclusion into a future version of LOWTRAN. Using the current LOWTRAN 6 Navy Maritime Aerosol Model as the surface kernel, this new model is intended to greatly reduce the third component's variation with altitude. The results of this study, however, have demonstrated that for moderate wind-speed conditions, the current wind-speed component in the kernel model may be factors near 20 too large. Therefore, a careful re-examination should be given to the constants of the present model before inclusion to NOVAM.

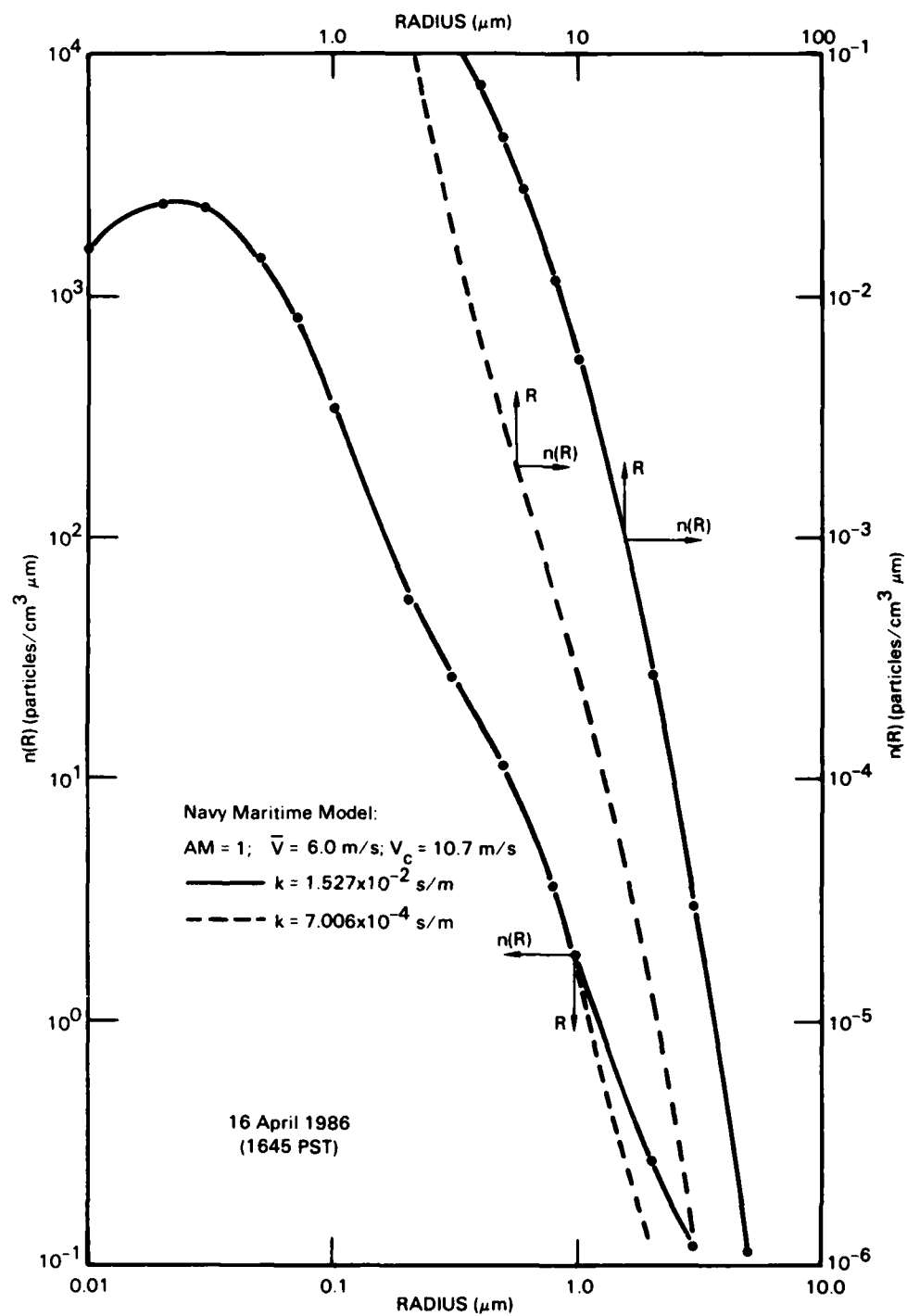


Figure 6. Examples of aerosol size distributions calculated with different values of the multiplying factor  $k$ .

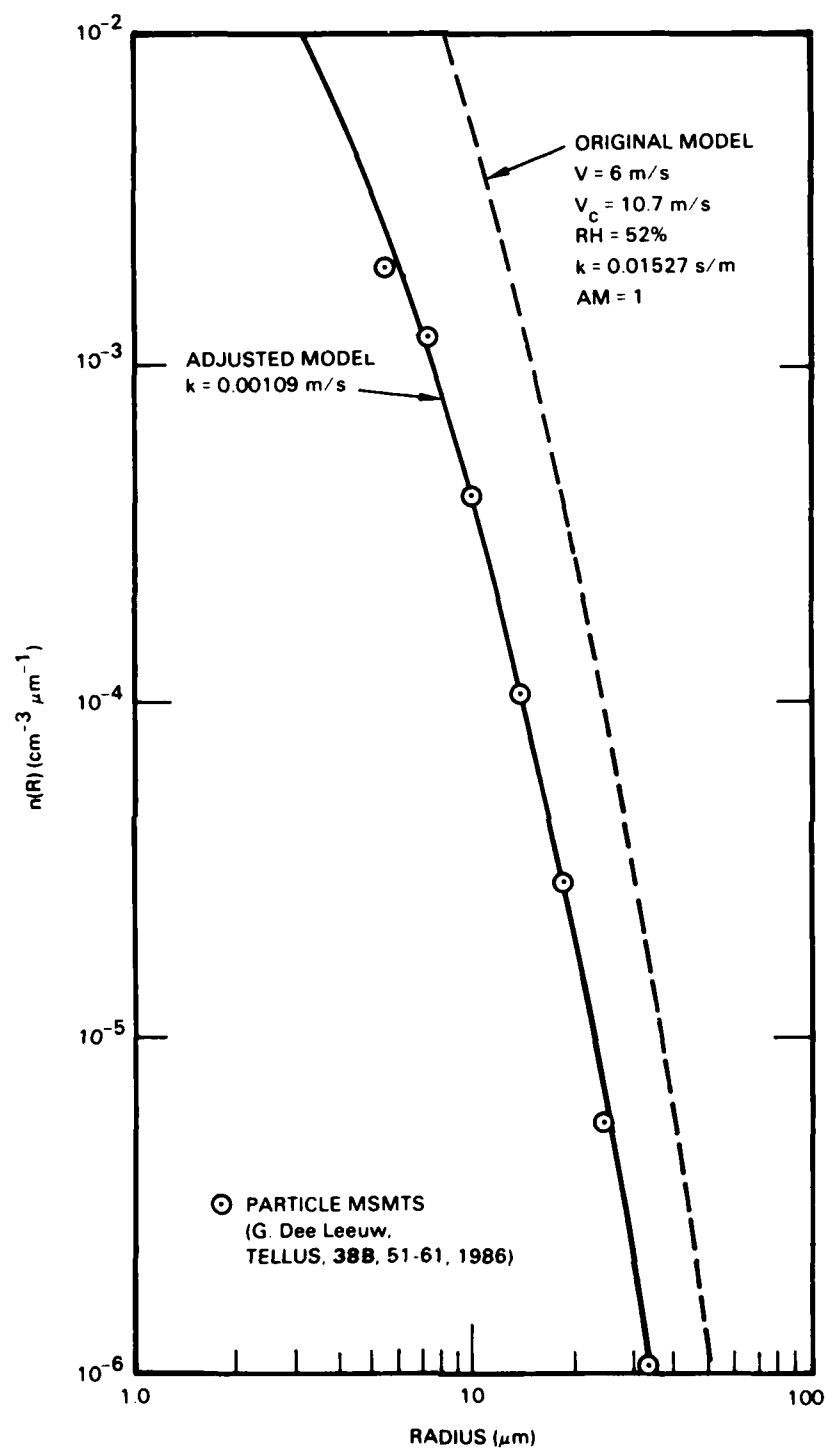


Figure 7. Comparisons of measured particle size distributions with those calculated with the original and adjusted Navy Maritime Aerosol Model.

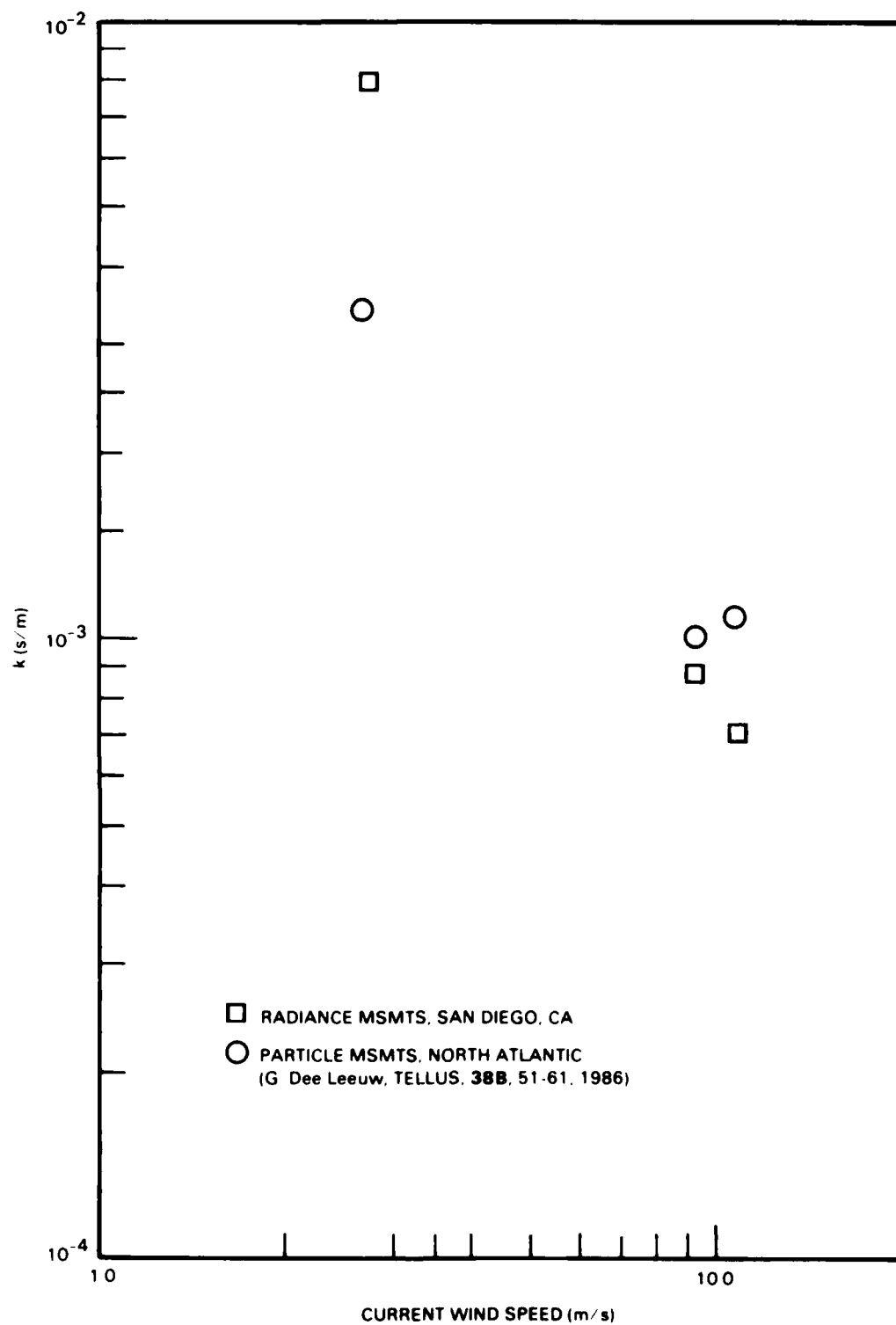


Figure 8. Values of the current wind-speed multiplying factor  $k$  required to obtain agreement between measured and calculated radiances and particle size distributions.

## REFERENCES

1. F.X. Kneizys, et al., "Atmospheric Transmittance/Radiance: Computer Code LOWTRAN 6," AFGL-TR-83-0187 (1983).
2. S.G. Gathman, "Optical Properties of the Marine Aerosol as Predicted by the Navy Aerosol Model," *Opt. Eng.*, 22, 57-62 (1983).
3. S.G. Gathman and B. Ulfers, "On the Accuracy of IR Predictions Made by the Navy Aerosol Model," American Meteorological Society Ninth Conference on Aerospace and Aeronautical Meteorology, June 6-9, 1983, Omaha, NE, pp. 194-198.
4. E.E. Bell, L. Eisner, J. Young and R.A. Oetjen, "Spectral Radiance of Sky and Terrain at Wavelengths Between 1 and 20 Microns. II. Sky Measurements," *J. Opt. Soc. Am.*, 50, pp. 1313-1320 (1960).
5. A.B. Barzilai Ben-Shalom, D. Cabib, A.D. Devir, S.G. Lipson and U.P. Oppenheim, "Sky Radiance at Wavelengths Between 7 and 14  $\mu\text{m}$ : Measurements, Calculation and Comparison with LOWTRAN-4 Predictions," *Appl. Opt.*, 19, pp. 838-839 (1980).
6. H.G. Hughes, W.J. Schade and L.R. Hitney, "Effects of Aerosols on Low-Elevation Infrared Sky Radiances," *Appl. Opt.*, 25, pp. 1536-1538 (1986).
7. H.G. Hughes, "LOWTRAN Modeling of Near-Horizon Infrared Sky Radiances in the Presence of Clouds," NOSC TD 988, September 1986.
8. G. Dee Leeuw, "Vertical Profiles of Giant Particles Close Above the Sea Surface," *TELLUS*, 38B, 51-61, 1986.
9. J.W. Fitzgerald, "Approximate Formulas for the Equilibrium Size of an Aerosol Particle as a Function of Its Dry Size and Composition and the Ambient Relative Humidity," *J. Appl. Meteor.*, 14, 1044-1049, 1975.

END

6-87

DTIC